ACS APPLIED MATERIALS & INTERFACES

Research Article

www.acsami.org

Methotrexate-Loaded Four-Arm Star Amphiphilic Block Copolymer Elicits CD8$^+$ T Cell Response against a Highly Aggressive and Metastatic Experimental Lymphoma

Sumit Kumar Hira,[†,⊥,∥] Kalyan Ramesh,[‡,§,∥] Uttam Gupta,[†] Kheyanath Mitra,[‡] Nira Misra,[§] Biswajit Ray,[*,‡] and Partha Pratim Manna[*,†]

[†]Immunobiology Laboratory, Department of Zoology, Faculty of Science, Banaras Hindu University, Varanasi 221005, India

[‡]Department of Chemistry, Faculty of Science, Banaras Hindu University, Varanasi 221005, India

[§]School of Biomedical Engineering, Indian Institute of Technology (Banaras Hindu University), Varanasi 221005, India

[⊥]Department of Zoology, The University of Burdwan, Burdwan 713104, West Bengal, India

Supporting Information

ABSTRACT: We have synthesized a well-defined four-arm star amphiphilic block copolymer [poly(DLLA)-*b*-poly(NVP)]$_4$ [star-(PDLLA-*b*-PNVP)$_4$] that consists of D,L-lactide (DLLA) and *N*-vinylpyrrolidone (NVP) via the combination of ring-opening polymerization (ROP) and xanthate-mediated reversible addition−fragmentation chain transfer (RAFT) polymerization. Synthesis of the polymer was verified by ^{1}H NMR spectroscopy and gel permeation chromatography (GPC). The amphiphilic four-arm star block copolymer forms spherical micelles in water as demonstrated by transmission electron microscopy (TEM) and ^{1}H NMR spectroscopy. Pyrene acts as a probe to ascertain the critical micellar concentration (cmc) by using fluorescence spectroscopy. Methotrexate (MTX)-loaded polymeric micelles of star-(PDLLA$_{15}$-*b*-PNVP$_{10}$)$_4$ amphiphilic block copolymer were prepared and characterized by fluorescence and TEM studies. Star-(PDLLA$_{15}$-*b*-PNVP$_{10}$)$_4$ copolymer was found to be significantly effective with respect to inhibition of proliferation and lysis of human and murine lymphoma cells. The amphiphilic block copolymer causes cell death in parental and MTX-resistant Dalton lymphoma (DL) and Raji cells. The formulation does not cause hemolysis in red blood cells and is tolerant to lymphocytes compared to free MTX. Therapy with MTX-loaded star-(PDLLA$_{15}$-*b*-PNVP$_{10}$)$_4$ amphiphilic block copolymer micelles prolongs the life span of animals with neoplasia by reducing the tumor load, preventing metastasis and augmenting CD8$^+$ T cell-mediated adaptive immune responses.

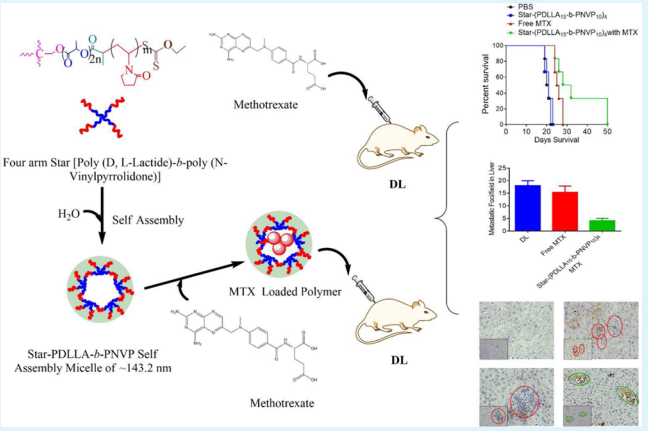

KEYWORDS: *methotrexate, star-[poly(DLLA)-b-poly(NVP)]$_4$, drug resistance, drug delivery, hemocompatibility, lymphoma*

INTRODUCTION

Polymeric micelles containing a hydrophobic core and a hydrophilic shell are usually formed following self-assembling of amphiphilic block copolymers (ABCs) in water and are used as an excellent nanocarrier in pharmacological applications as well as in sensing and image enhancement.[1] Drug-loaded micelles have higher permeability and retention (EPR) effect.[2] Coating the surface of the drug-loaded hydrophobic polylactide-based nanoparticles (NPs) with hydrophilic polymers is one promising approach to achieving long circulation in the blood.[3] In recent years, star-like amphiphilic block copolymers have attracted attention because of their unique solution and solid-state properties.[4−7] Our group has shown the synthesis of amphiphilic diblock and star block copolymers of ε-caprolactone (CL) and *N*-vinylpyrrolidone (NVP) via the union of controlled ring-opening polymerization (ROP) of CL and xanthate-mediated reversible addition−fragmentation chain transfer (RAFT) polymerization of NVP.[8,9] NVP having a nonconjugated amide keto group connected to a vinyl group can be polymerized only by radical polymerization.[10−14] ABCs with a hydrophobic poly(D,L-lactide) (PDLLA) are biocompatible and biodegradable, which makes them highly significant with respect to their application in industry and medical science.[15,16]

Hydrophilic PNVP in combination with hydrophobic PDLLA forms an amphiphilic block copolymer micelle, which

Received: June 4, 2015
Accepted: August 25, 2015
Published: August 25, 2015

DOI: 10.1021/acsami.5b04905
ACS Appl. Mater. Interfaces 2015, 7, 20021−20033

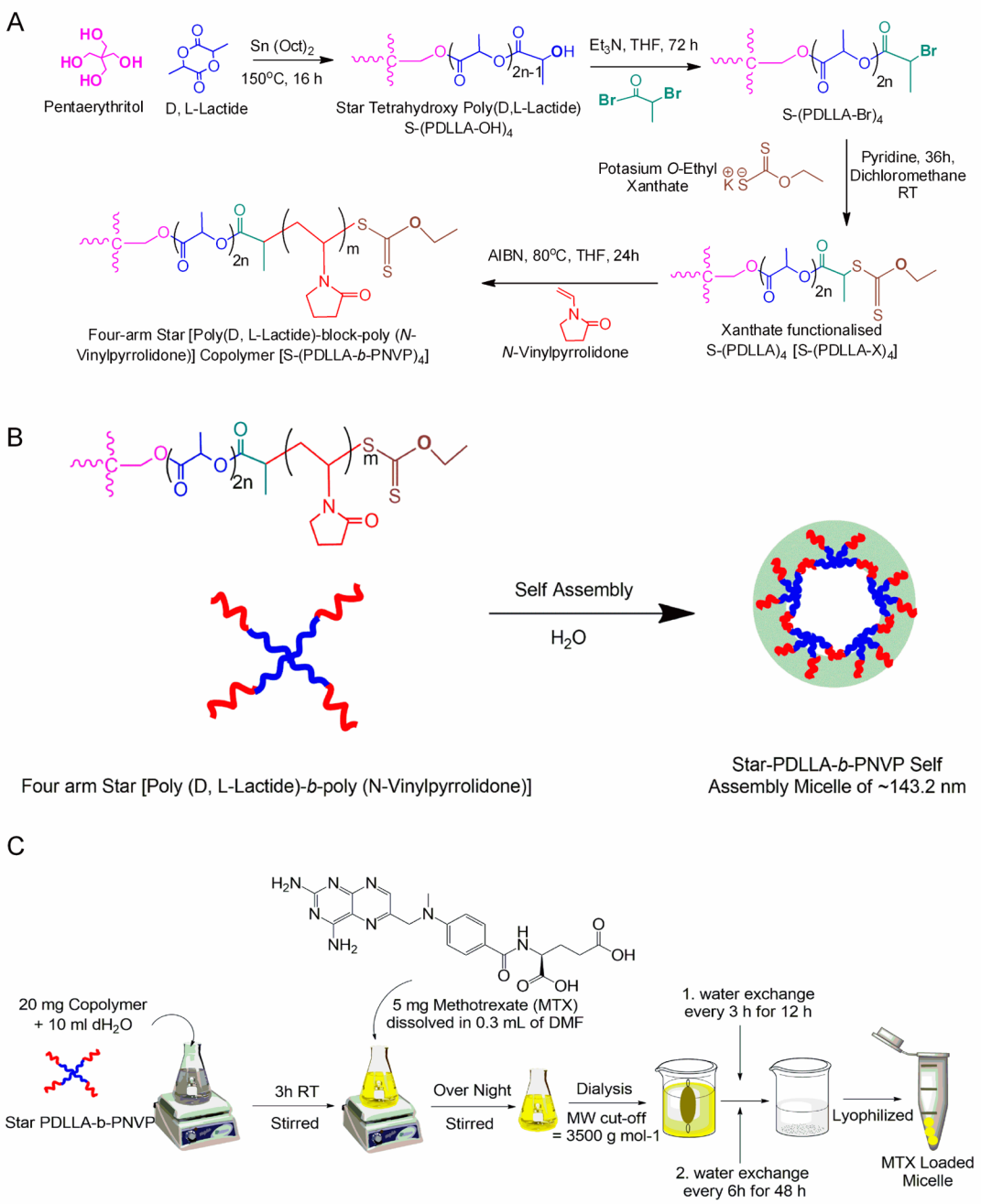

Figure 1. Formation of MTX-loaded sar-(PDLLA$_{15}$-*b*-PNVP$_{10}$)$_4$: (A) diagrammatic presentation of the synthesis of four-arm star poly(D,L-lactide)-*b*-poly(*N*-vinylpyrrolidone) copolymer [S-(PDLLA-*b*-PNVP)$_4$] via the combination of ROP and xanthate-mediated RAFT polymerization; (B) diagrammatic presentation for the generation of micelles; (C) detailed illustration for the formation of MTX-loaded S-(PDLLA$_{15}$-*b*-PNVP$_{10}$)$_4$.

is an attractive platform for delivering hydrophobic drugs.[17] Recently, our group has reported the synthesis of amphiphilic diblock copolymers of DLLA and NVP.[18] Synthesis of star-shaped poly(DL-lactide)-*b*-poly(ethylene glycol) by ROP has been reported by using diverse contents of pentaerythritol in association with a stannous octoate [(Sn(Oct)$_2$] catalyst, where it condensed with carboxyl-terminated poly(ethylene glycol) methyl ether.[19] Wei et al.[20] have reported the synthesis of star-shaped block copolymers of PLLA-*sb*-poly[*N*-isopropylacrylamide (NIPAAm)-*co*-*N*-hydroxymethylacrylamide (HMAAm)] with varied molar feed ratios of NIPAAm. An amphiphilic and double-responsive star-block copolymer has been synthesized by Li et al. via RAFT polymerization of *N*,*N*-dimethylaminoethyl methacrylate (DMAEMA) from the star-shaped macro-RAFT agent, which was made by attaching a 3-benzyl sulfanyl thiocarbonyl sulfanyl propionic acid (BSPA)-terminated five-arm star PCL-*b*-PLLA polymer.[21] Later, Fischer et al.[22] reported a quick one-pot two-step synthesis of PLLA multiarm stars, based on a hyperbranched poly(glycolide) (hbPGA) copolymer core via solvent-free Sn(Oct)$_2$-catalyzed ROP.

Kang and Leroux[23] demonstrated the synthesis and self-assembling properties in water of novel A-B-A type triblock and star-shaped block amphiphilic copolymers of *N*-(2-hydroxypropyl) methacrylamide (HPMA) or *N*-vinyl-2-pyrrolidone (NVP) and DL-lactide (DLLA). These uncontrolled polymers were made via free radical polymerization of HPMA or NVP in

DOI: 10.1021/acsami.5b04905
ACS Appl. Mater. Interfaces 2015, 7, 20021−20033

Table 1. Synthesis of Four-Arm Star-(PDLLA-X)$_4$ Macrochain Transfer Agent

run	sample	conv (%)[a] (NMR%)	M_n(g mol^{-1}) NMR[a]	M_n(g mol^{-1}) GPC[b]	PDI[b] (GPC)	comments
1	S-(PDLLA$_{15}$-OH)$_4$[c]	92	3440	7000	1.24	unimodal
2	S-(PDLLA$_{15}$-Br)$_4$[d]	100	4640	5200	1.52	unimodal
3	S-(PDLLA$_{15}$-X)$_4$[e]	100	5160	8500	1.55	unimodal

[a]By ^{1}H NMR. [b]By GPC (DMF, 0.5 mL/min, 40 °C) calibrated against PMMA standards. [c]Bulk polymerization using 6.0 g (41.6 m mol) of LA, 30 mg (7.4 × 10^{-5} mol) of Sn(oct)$_2$) in the presence of pentaerythritol at 150 °C for 16 h. [d]Using S-(PDLLA-OH)$_4$/trimethylamine/2-bromopropionyl bromide 1:2.5:2 in THF at room temperature for 72 h. [e]Using S-(PDLLA-Br)$_4$/potassium *O*-ethyl xanthate/pyridine 1:3:53 in dichloromethane (DCM) at room temperature for 36 h.

association of novel thiol-terminated PDLLA chain transfer agents. So far there has been no report about the controlled synthesis of the corresponding four-arm star (BA)$_4$-type amphiphilic block copolymers. Here, we have prepared well-defined four-arm star (PDLLA-*b*-PNVP)$_4$ block copolymers and studied their self-assembly properties and application as nanocarriers for drug delivery.

Methotrexate (MTX) is an antimetabolite and antifolate drug, widely used against cancer.[24] MTX is a powerful inhibitor (K_i = 0.058 nM[16]), and competitively inhibits dihydrofolate reductase (DHFR), an enzyme that participates in tetrahydrofolate synthesis.[25] Although effective for treatment against certain cancers[24] and rheumatoid arthritis,[26] MTX has suffered restrictive use due to adverse side effects including hepatotoxicity, which led to its reduced therapeutic potential.[24] Targeted delivery of MTX offers a new strategy to facilitate its uptake by neoplastic cells, which could enhance its therapeutic index.[27] The approach is based on designing methods of delivering the therapeutic payloads directly to the cancer cells for maximum efficacy.[27,28]

Herein, we have demonstrated the synthesis of a well-defined four-arm star (PDLLA$_{15}$-*b*-PNVP$_{10}$)$_4$ [S-(PDLLA-*b*-PNVP)$_4$] block copolymer. Self-assembly properties of the star block copolymer were determined by ^{1}H NMR, fluorescence spectroscopy, and transmission electron microscopy. MTX-loaded block copolymer micelles of S-(PDLLA-*b*-PNVP)$_4$ were prepared and characterized by UV−vis and TEM. MTX-loaded star-(PDLLA$_{15}$-*b*-PNVP$_{10}$)$_4$ ABCs suppress lymphoma cells in vitro via apoptosis. MTX-loaded star-(PDLLA$_{15}$-*b*-PNVP$_{10}$)$_4$ ABCs also kill MTX-resistant (MTX-R) lymphoma cells, whereas free MTX remains ineffective. In addition, MTX-loaded ABCs inhibit the colony formation of tumor cells and do not cause hemolysis compared to free MTX, which is toxic for RBC. The MTX-loaded star system protects mice with Dalton's lymphoma (DL)[29] and prolongs the lifespan of mice by augmenting tumor-specific protective adaptive immune responses mediated via CD8$^+$ T cells.

RESULTS AND DISCUSSION

Synthesis of Four-Arm Star Block Copolymers S-(PDLLA-*b*-PNVP)$_4$. The synthesis of four-arm star-(PDLLA$_{15}$-*b*-PNVP$_{10}$)$_4$ block copolymers was performed by amalgamating the methods of ROP and xanthate-mediated RAFT polymerization (Figure 1A,B). In the first step, well-defined four-armed S-(PDLLA$_{15}$-OH)$_4$ was generated by ROP in bulk at 150 °C in the presence of Sn(Oct)$_4$ catalyst using the feed ratio of DLLA monomer and pentaerythritol initiator at 24 (run 1, Table 1). The ^{1}H NMR spectrum demonstrates its formation (Figure 2A). A unimodal GPC chromatogram with M_n (GPC) = 7000 g mol^{-1} and M_w/M_n = 1.24 was observed. The corresponding molecular weight calculated from its ^{1}H NMR [M_n (NMR)] was 3440 g mol^{-1} (Figure 2A). The observed higher molecular weight in GPC measurement could be due to the star shape of the polymer and the use of the PMMA standards for calibration. The OH end groups in S-(PDLLA-OH)$_4$ were then converted into its corresponding bromide S-(PDLLA$_{15}$-Br)$_4$ upon reaction with 2-bromopropionyl bromide in combination with triethylamine (run 2, Table 1). The appearance of methine (f) and methyl (g) protons of the 2-bromopropionyl end group of the PDLLA15-Br was at around 4.72 and 1.72 ppm, which indicates the incorporation of the 2-bromopropionyl group (Figure 2B). The percent conversion (%) of the OH end group into its corresponding 2-bromopropionyl end group was derived by comparing the peak area of methyl protons g of the 2-bromopropionyl end group with that of the methylene proton of the polymer chain end at ∼4.2 ppm, which was ∼100%. The M_n(NMR) of this polymer was determined by dividing average the peak area of methylene protons b of the PDLLA backbone chain by the peak area of a, which was 4640 g mol^{-1}. The corresponding documented unimodal GPC chromatogram has M_n (GPC) and PDI values of 5200 g mol^{-1} and 1.52, respectively. The S-(PDLLA$_{15}$-Br)$_4$ polymer was subsequently reacted with potassium-*O*-ethyl xanthate to transform the bromo end group into its corresponding xanthate [S-(PDLLA$_{15}$-X)$_4$] by ionic substitution reaction (run 3, Table 1). The appearance of a new peak of methylene proton f of the xanthate end group at 4.6 ppm confirms the formation of xanthate end group from the bromo end group (Figure 2C). The methyl proton h peaks of the xanthate end group and g peaks of the propionyl group are overlapped within the peaks of the methyl protons c of the PDLLA backbone chain. Comparison of the peak area of methine protons g of the propionyl group with the methylene protons f of the xanthate end group was ∼100%. This indicates the percent conversion of the Br end group to a xanthate end group as studied by ^{1}H NMR. The UV absorption peak of the −S—(C═S)− functional group of the xanthate chain end group of the star polymer S-(PDLLA$_{15}$-X)$_4$ was measured in its THF solution at $\lambda \sim 280$ nm. The M_n (NMR) value of the polymer was derived from ^{1}H NMR (Figure 2C) by dividing the peak area of b by the peak area of h and was calculated as 5160 g mol^{-1}. The corresponding observed unimodal GPC chromatogram has M_n (GPC) and PDI values of 8500 g mol^{-1} and 1.55, respectively.

RAFT polymerization of NVP mediated by xanthate was accomplished by using S-(PDLLA-X)$_4$ macrochain transfer agent with AIBN (1:1 molar ratio, in THF) at 80 °C for 24 h. The synthesis and characterization of S-(PDLLA-*b*-PNVP)$_4$ block copolymers are shown in Table 2. Runs 1, 2, and 3 (Table 2) indicate the 100, 200, and 300 equiv of NVP monomer loadings with respect to S-(PDLLA$_{42}$-X)$_4$ macrochain transfer agent. Unimodal GPC chromatograms were

DOI: 10.1021/acsami.5b04905
ACS Appl. Mater. Interfaces 2015, 7, 20021−20033

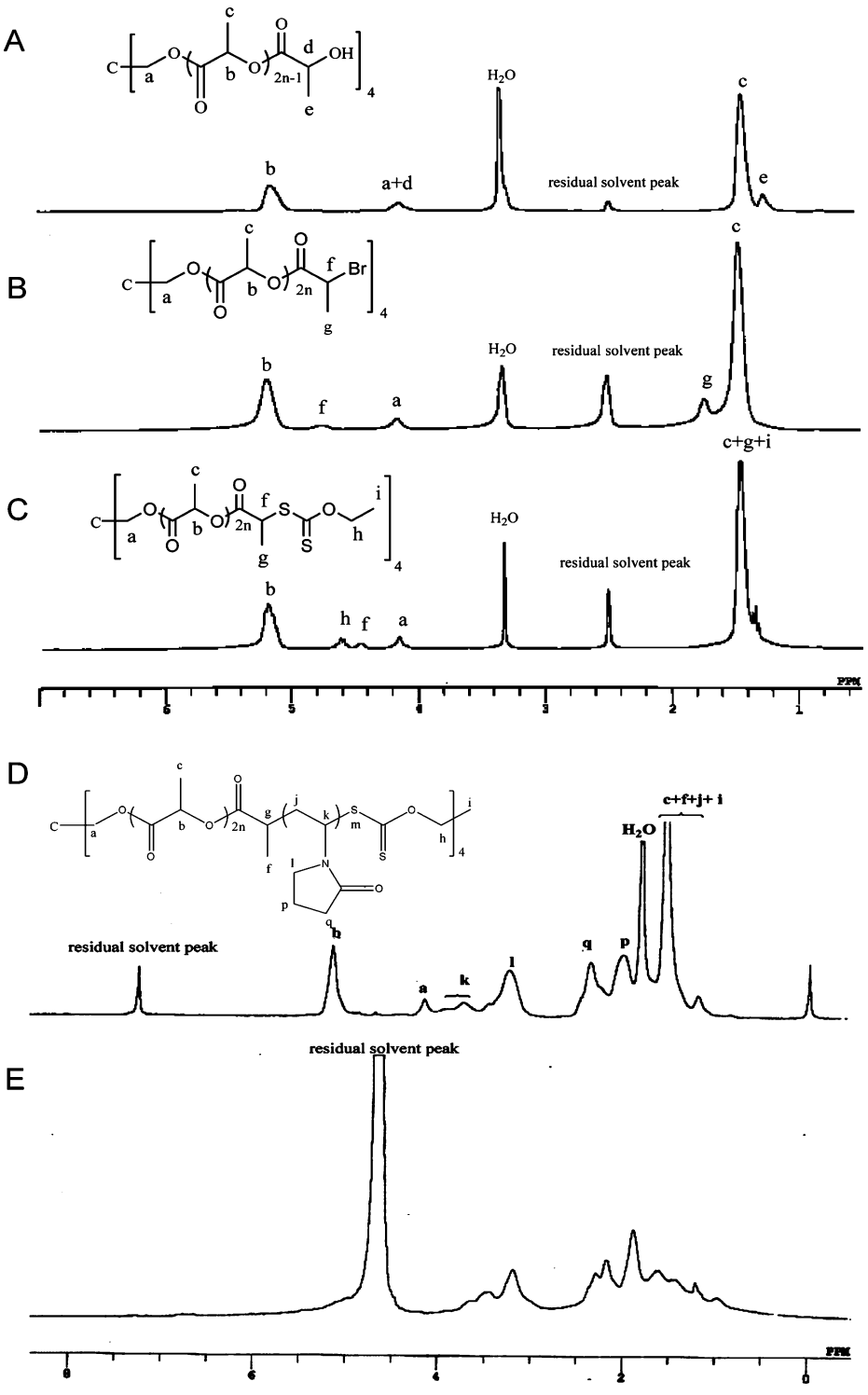

Figure 2. ^{1}H NMR spectra of (A) S-(PDLLA$_{15}$-OH)$_4$, (B) S-(PDLLA$_{15}$-Br)$_4$, and (C) S-(PDLLA$_{15}$-X)$_4$ in DMSO-d_6 at room temperature and ^{1}H NMR spectra of four-arm star block copolymer S-(PDLLA$_{15}$-*b*-PNVP$_{10}$)$_4$ in (D) *d*-chloroform and (E) D_2O at room temperature.

obtained. As expected, block copolymers have attained higher molecular weight due to the increase in monomer loading (Figure S1 in the Supporting Information).

^{1}H NMR and GPC studies of the mole fractions of PNVP blocks in copolymer were calculated in the range between 0.35 and 0.62. The block copolymers prepared in $CDCl_3$ in run 1 show (Table 2) the distinctive peaks of PDLLA block by ^{1}H NMR spectrum (Figure 2D). Besides that, it also shows the peaks of PNVP backbone methine proton k at ∼3.5−4.0 ppm, methylene protons i, q, and p of the pyrrolidone ring at ∼3.0−3.5, 2.2−2.5, and 1.8−2.2 ppm, respectively. Methylene proton j of the PNVP block overlapped between ∼1.2 and 1.8 ppm with the methyl proton c of PDLLA block. All star-block copolymers were completely soluble in water. All of these results indicate the successful occurrence of hetero chain extension.

Self-Assembly of Amphiphilic S-(PDLLA-*b*-PNVP)$_4$ Block Copolymers in Aqueous Solution. Amphiphilic

DOI: 10.1021/acsami.5b04905
ACS Appl. Mater. Interfaces 2015, 7, 20021−20033

Table 2. Details of S-(PDLLA-b-PNVP)$_4$ Block Copolymers[a]

run	block copolymer	NVP[b] (equiv)	conv[c] (NMR%)	M_n (g/mol) theor[d]	M_n (g/mol) NMR[e]	M_n (g/mol)/PDI[f] (GPC)	X_{NVP} GPC[g]	X_{NVP} NMR[g]	CMC[h] (mg/L)
1	S-(PDLLA$_{15}$-*b*-PNVP$_{10}$)$_4$	100	18.4	7200	9530	13200/1.32	0.35	0.46	3.64
2	S-(PDLLA$_{15}$-*b*-PNVP$_{14}$)$_4$	200	21.3	9900	12100	14900/1.25	0.43	0.57	5.14
3	S-(PDLLA$_{15}$-*b*-PNVP$_{15}$)$_4$	300	13.4	9630	13530	15400/1.24	0.44	0.62	5.81

[a]Using 1 equiv of AIBN with respect to S-(PDLLA$_{15}$-X)$_4$ macroinitiator in THF at 80 °C for 24 h. [b]With respect to S-(PDLLA$_{15}$-X)$_4$ macrochain transfer agent. [c]Conversion was determined by using ^{1}H NMR comparing the peak area of the residual vinylic segments of the NVP monomer at ∼4.3−4.4 ppm (^{2}H) and ∼7.0−7.1 ppm (^{1}H) with that of the methylene proton of the PNVP block of the polymer. [d]M_n (theor) = ^{1}H NMR mol wt of S(PDLLA$_{15}$-X)$_4$ + ([NVP]o/[S-(PDLLA$_{15}$-X)$_4$]o × fraction conversion of NVP (NMR) × mol wt of NVP). [e]Determined from ^{1}H NMR by comparing the peak area of the methylene protons of PDLLA block at ∼5.2 ppm with that of the methylene proton of PNVP block at ∼3.0−3.4 ppm. [f]Determined by GPC (DMF, 0.5 mL/min, 40 °C) calibrated against PMMA standard; g XPNVP = mole fraction of PNVP. [g]X_{PNVP} = mole fraction of PNVP. [h]CMC value determined by fluorescence spectroscopy.

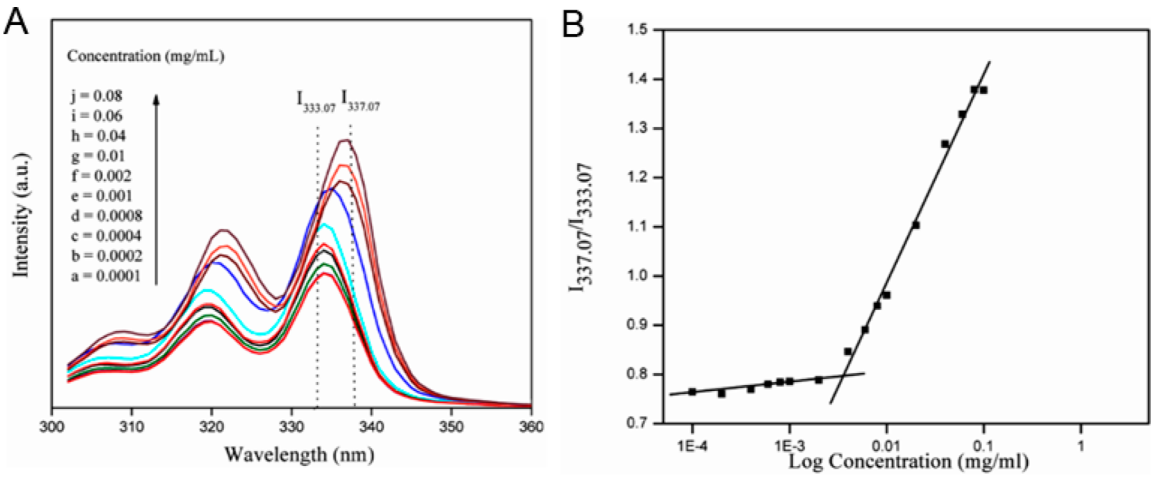

Figure 3. (A) Fluorescence excitation spectra (λ_{em} = 394 nm) of pyrene (6 × 10^{-7} M) in the presence of progressively higher concentrations (C) (mg/mL) of block copolymer S-(PDLLA$_{15}$-*b*-PNVP$_{10}$) (run 1, Table2) solution in water and (B) the corresponding semilogarithmic plot of the fluorescence excitation intensity ratio ($I_{337.07}/I_{333.07}$) of pyrene versus the concentration of the polymer.

block copolymers make nanostructures, which form clusters by assembling together (Figure 1B). The typical ^{1}H NMR spectrum of four-arm star block copolymer atar-(PDLLA$_{15}$-*b*-PNVP$_{10}$)$_4$ in D$_2$O has been described in Figure 2E. Here, the peaks attributed to PDLLA are suppressed compared to the results obtained in *d*-chloroform (Figure 2D). These results suggest the likely aggregation of micelles in water with PDLLA blocks acts as the core and PNVP blocks as the shell. ^{1}H NMR of the block copolymer in DMSO-d_6 is also shown (Figure S2). The critical micellar concentration (cmc) of the four-arm star block copolymers was studied in water by fluorescence spectroscopy using pyrene as a probe. The fluorescence spectra (300−360 nm) of pyrene (6 × 10^{-7} M) at different S-(PDLLA$_{15}$-*b*-PNVP$_{10}$)$_4$ (run 1, Table 2) concentrations were documented at a 394 nm emission wavelength (Figure 3A). Figure 3B exhibits the plot of the $I_{337.07}/I_{333.03}$ intensity ratio (fluorescence measurements) versus the log of the S-(PDLLA$_{15}$-*b*-PNVP$_{10}$)$_4$ block copolymer concentrations (mg/mL) in water. cmc values of the block copolymers S-(PDLLA$_{15}$-*b*-PNVP$_{10}$)$_4$, S-(PDLLA$_{15}$-*b*-PNVP$_{14}$)$_4$ (Figure S3), and S-(PDLLA$_{15}$-*b*-PNVP$_{15}$)$_4$ (Figure S4) are ∼3.64 × 10^{-3}, 5.14 × 10^{-3}, and 5.81 × 10^{-3} mg/mL, respectively (Table 2). The results suggest that as the PNVP block chain length increased, a corresponding augmentation of the cmc values of the amphiphilic block copolymer was noted. Identical observations were also made by other investigators.[8,18,30]

Methotrexate Loading and in Vitro Release Study. MTX is a synthetic compound used to treat leukemia and other forms of cancer and can be encapsulated inside the hydrophobic core of the polymeric micelle. The MTX-containing polymeric micelles were generated by using a dialysis method (Figure 1C). The amount of encapsulated MTX in polymeric micelle was determined from the absorbance of MTX at 308 nm. As expected, a TEM study (Figure 4A,B) clearly shows larger size for drug-loaded micelle (110 nm diameter) compared to unloaded micelle (32 nm diameter). These data suggest that star micelles were successfully loaded with MTX. The percent content and efficiency of MTX incorporation in star-(PDLLA$_{15}$-*b*-PNVP$_{10}$)$_4$ micelles were 6.0 and 31%, respectively. In vitro MTX release studies for the formulation were performed in PBS (pH 7.4 and 6.4) at 37 °C (Figure 4C). MTX-loaded micelles of star-(PDLLA$_{15}$-*b*-PNVP$_{10}$)$_4$ show sustained release behavior up to 40.5 and 23% at pH 6.4 and 7.4, respectively, during the initial 24 h. Slow drug release is critical for drug delivery when polymeric carriers can be delivered to the targeted tissue through the bloodstream during circulation. The chemical nature and composition of polymeric micelles significantly affect its drug release properties in vitro. The observed slow drug release in each case may result from mutual influence and interaction between hydrophobic MTX and hydrophobic PDLLA chain length.[31] The charges of the bare micelle and the drug-loaded micelle of star-(PDLLA$_{15}$-*b*-PNVP$_{10}$)$_4$ are −36.7 and −47.4 mV, respectively. The corresponding plots (Horiba SZ100 nanosizer) are shown in Figure S5.

DOI: 10.1021/acsami.5b04905
ACS Appl. Mater. Interfaces 2015, 7, 20021−20033

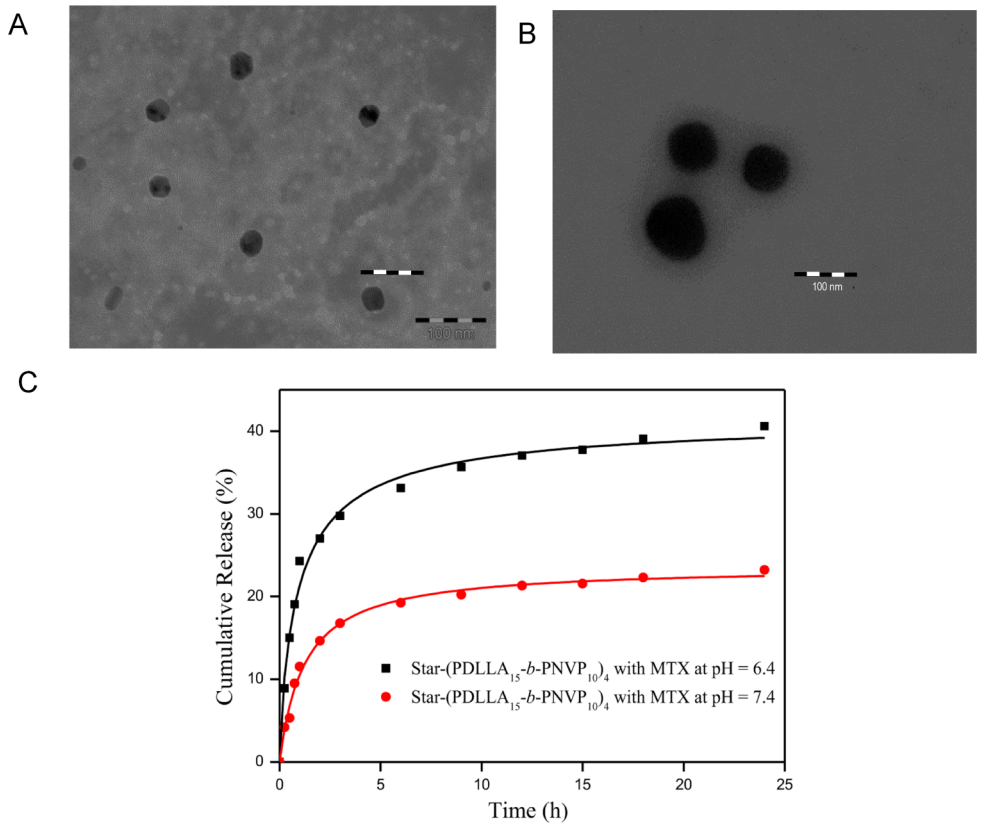

Figure 4. Transmission electron micrographs of (A) star-$(PDLLA_{15}$-*b*-$PNVP_{10})_4$ micelles and (B) MTX-loaded star-$(PDLLA_{15}$-*b*-$PNVP_{10})_4$ micelles. The magnification scale is the same for all micrographs. (C) Percentage of cumulative release of MTX from drug-loaded star-$(PDLLA_{15}$-*b*- $PNVP_{10})_4$ micelles in pH 6.4 and 7.4 PBS solution at 37 °C.

Effect of MTX-Loaded Star-$(PDLLA_{15}$-*b*-$PNVP_{10})_4$ on Tumor Cell Viability and Cytotoxicity. Compared to free MTX, MTX-loaded star-$(PDLLA_{15}$-*b*-$PNVP_{10})_4$ ABC significantly inhibited the cell viability of murine (DL) and human (Raji) lymphoma cells (Figure 5). A blend of MTX and polymer alone behaves similarly to MTX only. Compared to free MTX, parental DL (A) and Raji (C) cells are more susceptible in the presence of MTX-loaded star-$(PDLLA_{15}$-*b*-$PNVP_{10})_4$ ABCs, causing significant prevention in tumor cell viability (Figure 5A,C). In contrast, the MTX-resistant DL or Raji cells are tolerant to MTX but remain sensitive to MTX-loaded star copolymers (Figure 5B,D). Cell viability of DL and Raji cells remains unaffected by the carrier alone. An array of biodegradable polymers have been developed with enhanced intracellular drug release potential and capacity to respond to stimuli such as pH and temperature. These polymers are also capable of reversing multidrug resistance (MDR) in cancer cells.[32,33] Our result demonstrate that MTX-loaded star-$(PDLLA_{15}$-*b*-$PNVP_{10})_4$ ABC performs better in acidic pH, indicating its suitability to work inside the tumor cells (Figure 5). Susceptibility of tumor cells with respect to cellular cytotoxicity by MTX-loaded star-$(PDLLA_{15}$-*b*-$PNVP_{10})_4$ ABC is supportive of the above arguments (Figure 5E−H). Our results suggest that compared to MTX alone, MTX-loaded star-$(PDLLA_{15}$-*b*-$PNVP_{10})_4$ ABC kills tumor cells efficiently at all concentrations tested (Figure 5E,G). The carrier alone remains tolerant to the tumor cells and is not cytotoxic against either DL or Raji. Resistant variants of DL and Raji cells endure MTX but become sensitive to MTX-loaded star-$(PDLLA_{15}$-*b*-$PNVP_{10})_4$ ABCs at all concentrations tested (Figure 5F,H). MTX-loaded star-$(PDLLA_{15}$-*b*-$PNVP_{10})_4$ ABCs showed an antiproliferative effect and apoptosis against MTX-resistant tumor cells, indicating its effectiveness over the free MTX (Figures S6−S8). Direct comparisons of cell viability and cytotoxicity against the tumor cells by MTX-loaded star and linear copolymer suggest that the star compound is significantly more tumoricidal compared to its linear counterpart (Figure S9). MTX-loaded star-$(PDLLA_{15}$-*b*-$PNVP_{10})_4$ ABCs are significantly more efficient in long-term growth inhibition of parental and MTX-resistant tumor cells compared to linear copolymers (Figure S10). IC_{50} values of star-$(PDLLA_{15}$-*b*-$PNVP_{10})_4$ ABCs are significantly lower compared to the linear form in each case studied (Figure S10). Besides, that MTX-loaded star-$(PDLLA_{15}$-*b*-$PNVP_{10})_4$ ABCs prevent colony formation by DL and Raji cells significantly more highly than MTX alone (Figure S11). Survival analysis of DL and Raji cells suggests a sharp decline in free MTX starting at a concentration of 1−2 μM MTX compared to MTX-loaded star-$(PDLLA_{15}$-*b*-$PNVP_{10})_4$ copolymers (Figure S11).

MTX-Loaded Star-$(PDLLA_{15}$-*b*-$PNVP_{10})_4$ Is Tolerant to Normal Cells. Unlike tumor cells, normal human red blood cells (RBCs), lymphocytes, and dendritic cells (DCs) show tolerance to MTX-loaded star-$(PDLLA_{15}$-*b*-$PNVP_{10})_4$ ABCs (Figure 6). Hemolysis, studied at increasing time points and concentrations, suggests that MTX-loaded star-$(PDLLA_{15}$-*b*-$PNVP_{10})_4$ ABCs do not cause damage to RBCs compared to free MTX, which is significantly hemolytic (Figure 6A,B). The viability of DC and lymphocytes is unaffected by MTX-loaded ABCs (Figure 6C,D). In contrast, free MTX causes a significantly greater reduction in cell viability of lymphocytes

DOI: 10.1021/acsami.5b04905
ACS Appl. Mater. Interfaces 2015, 7, 20021−20033

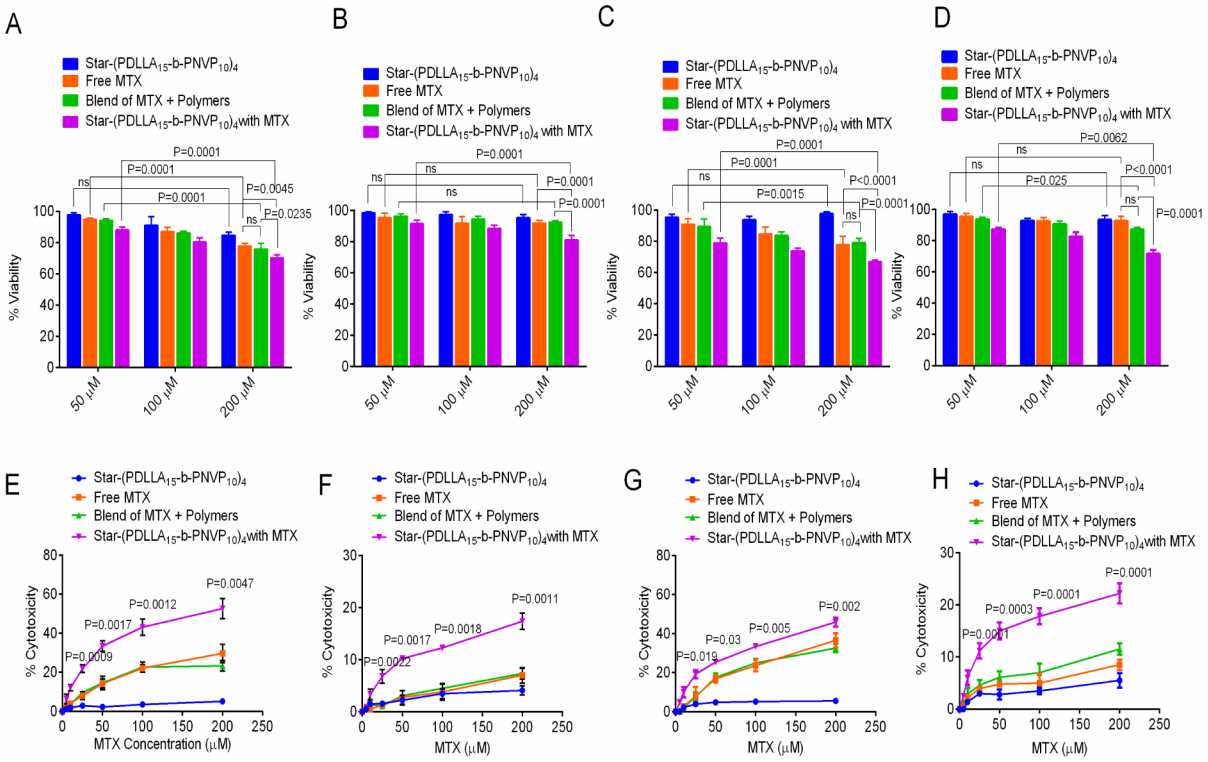

Figure 5. Loss of tumor cell viability and enhanced cytotoxicity by star-(PDLLA$_{15}$-*b*-PNVP$_{10}$)$_4$. (A, C) Viability of parental DL and Raji and (B, D) MTX-resistant DL and Raji cells was determined by XTT-based assay (Cell Signaling, Beverly, MA, USA). 5×10^3 cells were seeded in 96-well tissue culture plates containing complete medium in the presence or absence of free polymer, MTX, blend of MTX and polymer, or MTX-loaded polymeric micelles for 24 h at 37 °C with 5% CO_2. The cell viability of treated groups was quantified by assuming the tumor cells cultured in medium alone as 100%. An 18 h LDH release assay was used to determine the direct cell lysis by MTX-loaded star polymeric micelles against parental or MTX-resistant DL (E, F) or Raji cells (G, H). Data presented are the mean ± SD of triplicate determinations, $n = 4$ (n indicates the number of experiments performed).

and DCs at all concentrations of MTX (% lymphocytes viability 60.87 vs 93.26 at 1 mM concentration, $p < 0.0001$) (Figure 6C,D). Besides that, significantly higher cytotoxicity was observed in lymphocytes or DCs upon treatment with free MTX compared to MTX-loaded copolymer at all molar concentrations tested (Figure 6E,F). These results suggest that RBCs and normal immune cells are safe in the presence of MTX-loaded star-(PDLLA$_{15}$-*b*-PNVP$_{10}$)$_4$ ABC, whereas free MTX significantly harms their potential. The tolerance exhibited by DCs to MTX-loaded copolymers compared to free MTX is significant with reference to preservation of intact immune response mediated by DC, critical for effective therapeutic response in vivo. Similar to star-(PDLLA$_{15}$-*b*-PNVP$_{10}$)$_4$ ABCs, linear copolymers are also tolerated by normal human RBCs, lymphocytes, and DCs (Figure S12). Microscopic observations also demonstrate no change in morphology in RBCs following contact with the MTX-loaded star-(PDLLA$_{15}$-*b*-PNVP$_{10}$)$_4$ ABCs (Figure S13).

Increased Survival and Prevention of Metastasis by MTX-Loaded Star-(PDLLA$_{15}$-*b*-PNVP$_{10}$)$_4$ against DL Lymphoma. The therapeutic efficacy of MTX-loaded star-(PDLLA$_{15}$-*b*-PNVP$_{10}$)$_4$ ABC was studied in mice with DL.[34] DL tumors were transplanted into the peritoneum of female (4−6 weeks old) mice distributed in five different groups containing 12 mice each, and each was given six intravenous (iv) injections of (i) PBS, (ii) MTX alone (3 mg/kg body weight), (iii) polymer only (vehicle), or (iv) MTX-loaded star-(PDLLA$_{15}$-*b*-PNVP$_{10}$)$_4$ block copolymer (3 mg/kg of MTX) every 72 h. Therapy was started at 96 h post-tumor transplant (day 0) (Figure 7A). The animals given PBS or polymer alone developed tumors by day 12, which continued to increase in size as judged by the circumference of the peritoneum. MTX-treated mice also formed tumors and developed ascitis by day 20. MTX-loaded star-(PDLLA$_{15}$-*b*-PNVP$_{10}$)$_4$ ABC treated mice developed tumors at less than usual speed and formed tumors after day 25. Mice treated with PBS or control polymer succumbed to their death at day 22. MTX-treated mice were also unable to survive in excess of 25 days. In contrast, nearly 33% of mice (4 of 12 mice) treated with MTX-loaded star-(PDLLA$_{15}$-*b*-PNVP$_{10}$)$_4$ ABC survived beyond day 50, when final data collection was made. Mice treated with MTX-loaded star-(PDLLA$_{15}$-*b*-PNVP$_{10}$)$_4$ demonstrate significantly higher survival potential compared to MTX treatment alone as suggested by Kaplan−Meier survival analysis (Figure 7B). This observation was also supported by a reduction in abdominal circumference in MTX-loaded star-(PDLLA$_{15}$-*b*-PNVP$_{10}$)$_4$-treated mice. The average body weight of MTX-loaded star-(PDLLA$_{15}$-*b*-PNVP$_{10}$)$_4$-treated mice (26 g) is significantly lower than that of the mice treated with polymer control (38 g) or free MTX (35 g) (Figure 7C,D). Treatment with MTX-loaded star-(PDLLA$_{15}$-*b*-PNVP$_{10}$)$_4$ ABC results in a significant reduction in tumor burden, suggesting a favorable therapeutic index for the indicated formulation. The above formulation significantly restricts the metastasis of tumor cells in the liver as suggested by histopathology study (Figure 7E). As shown in Figure 7E, the metastatic infiltrates (red circle) are significantly decreased in the liver following treatment with MTX-loaded star-(PDLLA$_{15}$-*b*-PNVP$_{10}$)$_4$. The numbers of

DOI: 10.1021/acsami.5b04905
ACS Appl. Mater. Interfaces 2015, 7, 20021−20033

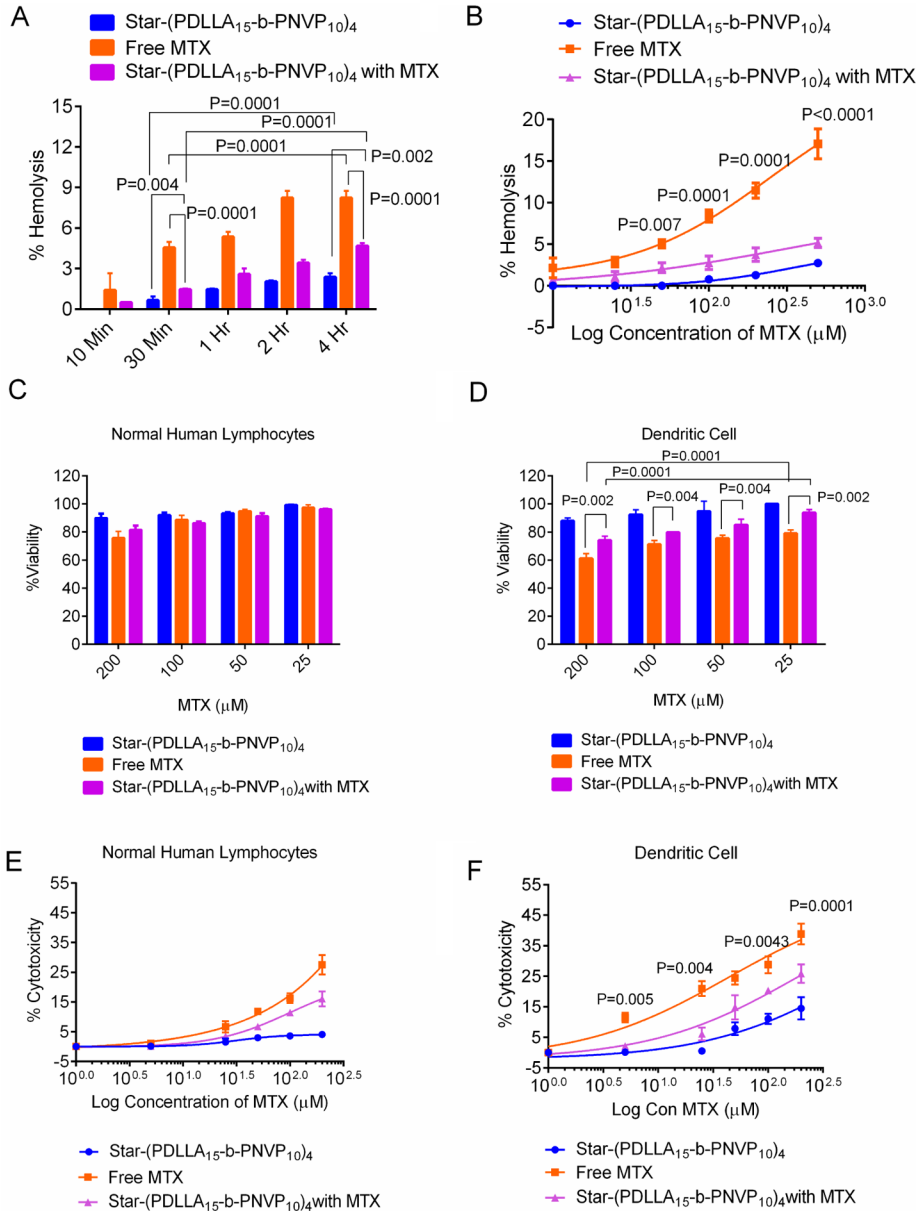

Figure 6. MTX-loaded star-(PDLLA$_{15}$-*b*-PNVP$_{10}$)$_4$ micelles are tolerant to RBCs and lymphocytes: lysis of RBC by MTX or MTX-loaded star copolymer following incubation at different time points (A) or in the presence of various concentrations of the formulations (B). Data are expressed as percent hemoglobin content in RBC, mean ± SD, n = 3. Normal human lymphocytes (C) and DCs (D) were given the indicated treatment in complete medium. XTT assay (Cell Signaling) was used to measure the cell viability. Representative data are expressed as the mean ± SD, n = 3. An 18 h LDH release assay demonstrated the cytotoxicity of leukocytes (E, F). Representative data are shown as the mean ± SD, n = 4.

metastatic field and metastatic foci were significantly diminished in the liver of mice treated with MTX-loaded star-(PDLLA$_{15}$-*b*-PNVP$_{10}$)$_4$ (p = 0.0005 between MTX and treatment in the liver) (Figure 7F). Star-(PDLLA$_{15}$-*b*-PNVP$_{10}$)$_4$ ABC demonstrate significantly better therapeutic efficacy compared to its linear counterpart (Figure S14). Long-term survival of tumor-bearing mice was higher following treatment with star-(PDLLA$_{15}$-*b*-PNVP$_{10}$)$_4$ ABCs with reduced body weight and abdominal circumference compared to similar treatment with linear copolymers (Figure S14).

Generation of CD8$^+$ T Cell Immunity in Treated Mice Following Therapy. Cytotoxic (CD8$^+$) T cells derived from the animals treated with MTX-loaded star-(PDLLA$_{15}$-*b*-PNVP$_{10}$)$_4$ ABC proliferate in response to DL antigen-stimulated dendritic cells, suggesting the improvement in T cell mediated adaptive immunity. This could be responsible for the partial therapeutic efficacy as observed in treated mice (Figure 8A–C). CD8$^+$ T cells from surviving mice kill DL target cells at a significantly higher rate compared to naïve CD8$^+$ T cells, suggesting that therapy induces the adaptive immune response against the tumor cells in vivo (Figure 8D). In addition, the treated group also demonstrates the high surge of CD8$^+$ T cells in the liver (green circle) with significantly less metastasis compared to untreated DL tumor-bearing mice (Figure 8E).

CONCLUSION

Methotrexate-loaded star-(PDLLA$_{15}$-*b*-PNVP$_{10}$)$_4$ polymeric micelles of amphiphilic block copolymer shows significant growth inhibition, cytotoxicity, and apoptosis of DL and Raji

DOI: 10.1021/acsami.5b04905
ACS Appl. Mater. Interfaces 2015, 7, 20021−20033

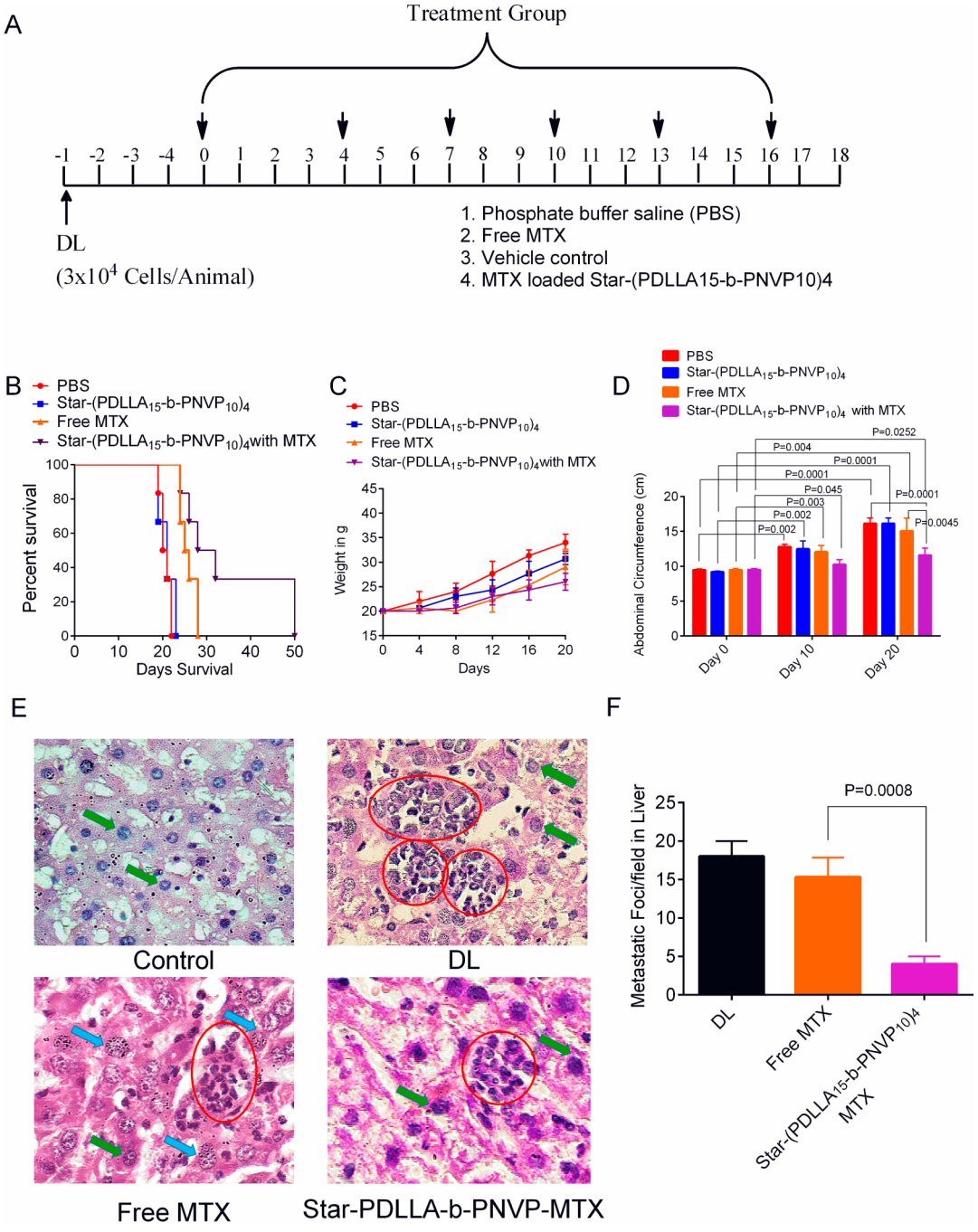

Figure 7. In vivo antitumor role of MTX-loaded star-$(PDLLA_{15}$-*b*-$PNVP_{10})_4$ micelles. Mice with DL tumors were given six doses of free MTX, polymer alone, or MTX-loaded star-$(PDLLA_{15}$-*b*-$PNVP_{10})_4$ micelles for 3 weeks (MTX dose of 3 mg/kg body weight) (A). Kaplan−Meier survival analysis was used to determine the percent survival up to day 50 post-tumor transplant by log-rank test using Graph Pad PRISM software (B). Body weight (C) and abdominal perimeter (D) were determined for the indicated treatment. Images of hematoxylin and eosin (H&E) staining of liver tissues derived from healthy control, untreated, mice with tumor or surviving group (E). Metastatic foci are shown in histology of liver sections (red circle). Tumor metastatic foci/fields (arrows) (F) were counted in untreated mice and in mice with indicated treatment.

cells. Star ABC also exhibits antitumor activity against MTX-resistant DL and Raji cells, whereas free MTX is ineffective. The formulation does not cause hemolysis of RBCs compared free MTX. Treatment of DL tumor-bearing mice with MTX-loaded star-$(PDLLA_{15}$-*b*-$PNVP_{10})_4$ ABC prolonged the survival of mice with active disease and generated the $CD8^+$ T cell-mediated cytolytic responses against DL, which was significantly impaired in untreated tumor-bearing mice. Compared to linear copolymer, the star form demonstrates superior performance with reference to antitumor activity.

EXPERIMENTAL PROCEDURES

Ethics Statement. This study was carried out in strict compliance with the recommendations for the care and use of laboratory animals of the National Regulatory Guidelines issued by the Committee for the Purpose of Supervision of Experiments on Animals (CPSEA), Ministry of Environment and Forest, Government of India. The protocol was approved by the Institutional Animal Ethics Committee, Banaras Hindu University. Mice were euthanized by cervical dislocation to reduce suffering to a minimum and was executed as per the AVMA Guidelines on Euthanasia (AVMA 2013).

DOI: 10.1021/acsami.5b04905
ACS Appl. Mater. Interfaces 2015, 7, 20021−20033

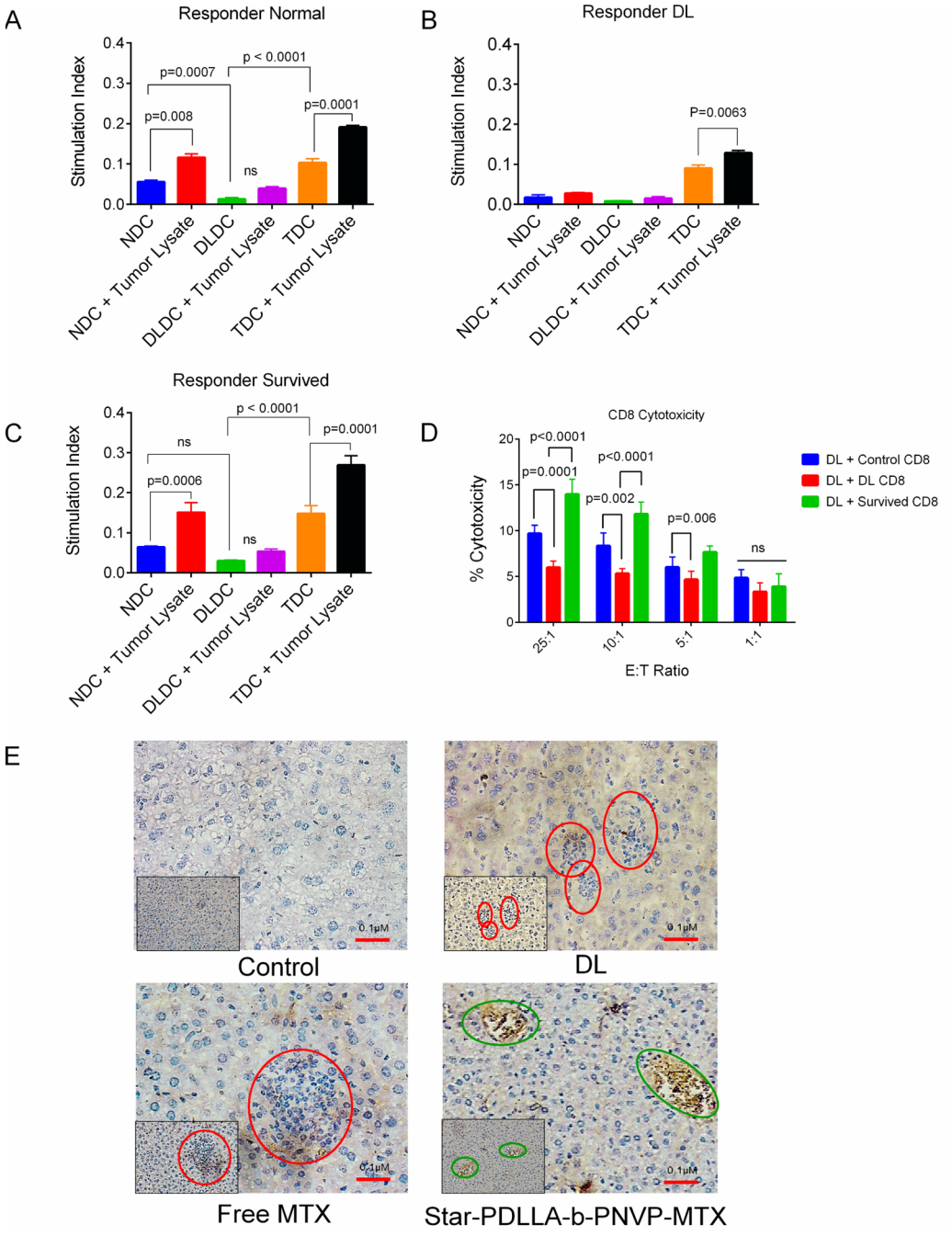

Figure 8. Development of $CD8^+$ adaptive immunity in treated mice. $CD8^+$ T cells from healthy control (A) DL tumor-bearing mice (B) and mice surviving after therapy with MTX-loaded star-$(PDLLA_{15}$-*b*-$PNVP_{10})_4$ (C) were used as responder cells in the presence of whole tumor lysate pulsed mitomycin C treated DC (stimulator) derived from the respective groups. Results are presented as antigen-specific proliferation and represented as the ratio of the proliferation of cytotoxic ($CD8^+$) T cells in the presence or absence of the tumor lysate pulsed DC from three different sources mentioned above. $CD8^+$ T cells (D) were used as effector cells against the DL tumor cells at multiple E:T ratios. Cytotoxicity was measured as mentioned above ($p < 0.0001$ between DL mice treated with or without MTX-loaded star-$(PDLLA_{15}$-*b*-$PNVP_{10})_4$). Mean ± SD, $n = 3$. (E) Immunohistochemical analysis of $CD8^+$ T cells in untreated and treated mice. Red circles represent the metastasized DL cells, and green circles represent the infiltration of $CD8^+$ T cells in the treated group, $n = 4$.

^{1}H NMR Study. ^{1}H NMR was performed at room temperature in a JEOL AL300 FTNMR (300 MHz) using $CDCl_3$ or D_2O as solvent. The % NVP monomer conversion was ascertained by ^{1}H NMR spectroscopy in $CDCl_3$.[15] A detailed methodology is given in the Supporting Information and Methods.

Fluorescence Experiments. Fluorescence studies were performed in a Varian Cary Eclipse fluorescence spectrometer. A range of concentrations of PDLLA-*b*-PNVP star block copolymer in water (5×10^{-3} to 1 mg/mL) was used for this purpose. Other details are given in the Supporting Information and Methods.

Transmission Electron Microscopy (TEM) and UV–Visible Study. The size of MTX-loaded or free polymeric micelles was measured by using TEM (JEOL, JEM, 2100) operated at an acceleration voltage of 120 kV. Samples were made by placing one drop of test solution (1 mg/mL) in a copper grid coated with carbon. Extra solution was removed by using a filter paper.

DOI: 10.1021/acsami.5b04905
ACS Appl. Mater. Interfaces 2015, 7, 20021−20033

Synthesis of Four-Arm Star-Poly(D,L-lactide) [S-(PDLLA$_{15}$-OH)$_4$]. A detailed methodology for the synthesis of four-arm star-poly(D,L-lactide) [S-(PDLLA$_{15}$-OH)$_4$] is described in the Supporting Information and Methods.

MTX Loading and in Vitro Release Study. Methotrexate (MTX) was loaded in star-(PDLLA-*b*-PNVP)$_4$ ABCs as reported earlier.[31] Details of the methodology are described in the Supporting Information and Methods.

For in vitro drug release assay, MTX-loaded polymeric micelles (5 mg) were dispersed in 2.0 mL of PBS (pH 7.4 and 6.4) and packed into a dialysis bag (MW cutoff = 3500 g mol^{-1}). A membrane with such a molecular weight cutoff allows only the drug to pass through and allows the retaining of polymer only. The dialysis bag was kept in a beaker containing PBS (50 mL) with constant temperature maintained at 37 °C. The system was stirred at 60 rpm. Two milliliters of PBS was removed from the beaker at regular intervals and was replenished with an equal amount of fresh PBS. MTX release from micelles was determined by UV spectroscopy at 308 nm.

Cell Lines, Cell Culture, and Development of MTX-Resistant DL and Raji Cells. Human Burkitt's lymphoma cell line Raji was originally procured from American Type Culture Collection (ATCC), Manassas, VA, USA. DL cells were transplanted intraperitoneally in AKR (H2k) mice as described before.[34] The tumor cells were cultured in RPMI 1640 (Invitrogen, Carlsbad, CA, USA) with supplements including 10% fetal bovine serum (Hyclone, Logan, UT, USA), 100 U/mL penicillin, and 100 μg/mL streptomycin (Invitrogen). This culture medium was considered as complete medium. All of the tumor cells were devoid of mycoplasma.

MTX-insensitive DL and Raji cells were generated and maintained according to the method demonstrated by Ohnoshi et al.[35] Details of the methodology are described in the Supporting Information and Methods. Peripheral blood lymphocytes and DCs were generated as described earlier.[36]

In Vitro Cell Viability, Proliferation, and Cytotoxicity Assay. Cell viability, cytotoxicity, and proliferation were performed as described before.[36] Details of the methodology are described in the Supporting Information and Methods.

Detection of Apoptosis. Detection of apoptosis in tumor cells in the presence of MTX-loaded star-(PDLLA$_{15}$-*b*-PNVP$_{10}$)$_4$ ABC was performed as described before.[36] Details of the methodology are described in the Supporting Information and Methods.

Clonogenic Survival Assay. The clonogenic survival assay and analysis of survival fractions of tumor cells cocultured with MTX-loaded star-(PDLLA$_{15}$-*b*-PNVP$_{10}$)$_4$ ABC was performed as described before.[36] Details of the methodology have been given in the Supporting Information and Methods.

Hemolysis Assay. Lysis of RBCs was determined according to the protocol described by Kuznetsova et al. with modifications.[37] Details of the methodology are described in the Supporting Information and Methods.

In Vivo Therapeutic Study. DL tumor cells (3×10^4 cells/mouse) in PBS were transplanted in the peritoneum of AKR/J mice and were kept for 4 days to develop tumors. Development of tumor was ascertained and assessed by measuring the abdominal perimeter. Mice (n = 12/group) were administered intravenously with free MTX, MTX-loaded star-(PDLLA$_{15}$-*b*-PNVP$_{10}$)$_4$ ABCs (3 mg/kg body weight), or empty copolymer micelles in PBS after 96 h (day 0), following tumor transplant. A total of six injections were administered with an interval of 72 h between the doses. The formulations were prepared and validated so that 100 μL of PBS (vehicle) contained 3 mg/kg body weight of MTX in MTX-loaded star-(PDLLA$_{15}$-*b*-PNVP$_{10}$)$_4$ ABC micelles. The animals were watched regularly, and the abdominal perimeter and body weights were documented. Three animals from each experimental group were sacrificed for midterm analysis of therapeutic performance when the mean abdominal perimeter of the PBS only group surpassed 15.5 cm. The remaining animals were maintained up to day 50 for survival analysis and performing experiments on T cell-mediated immune response.

Antigen-Specific T Cell Proliferation. CD8$^+$ T cells from normal (healthy control), DL tumor-bearing mice, or surviving treated mice were used as responder cells against the whole DL tumor lysate (10 μg/mL) pulsed and mitomycin C (10 μg/mL) treated stimulator DC, derived from healthy control, DL tumor-bearing mice, or surviving treated mice. The responder T cells (5×10^5) were cocultured with stimulator DC (5×10^3), and the culture plates were incubated at 37 °C with 5% CO_2 for 120 h, followed by MTT assay to assess the cell proliferation. The cell proliferation was measured as stimulation index (SI) calculated by dividing the mean OD of responder cells stimulated with tumor lysate pulsed DC by the mean OD of unstimulated responder cells only: stimulation index (SI) = experimental OD_{570}/control OD_{570}, where experimental OD represents the proliferation of responder T cells in the presence of DCs from normal (NDC), tumor-bearing mice (DLDC), or treated mice (TDC) stimulated with or without whole tumor cell lysate and control OD represents the proliferation of responder T cells only recorded at 570 nm.

Cytotoxicity Assay by CD8$^+$ T Cells Derived from Treated Mice. The cytotoxicity of CD8$^+$ T cell was determined by 18 h nonradioactive cytotoxicity assay as mentioned above.[38] Target cells (DL) and CD8$^+$ effector T cells (5×10^3) were cocultured in a flat-bottom 96-well plate at different E:T ratios and incubated for 18 h at 37 °C with 5% CO_2. Free LDH in supernatant liquid was quantified as described above.

Statistical Analysis. For each experimental group, the mean ± SD was calculated using the data collected from individual experiments (n = 3−5). Unpaired Student's t test and one- or two-way ANOVA analysis of variance were performed on the basis of demand. This was followed by Holm−Sidak post hoc multiple-comparison tests using PRISM statistical analysis software (GraphPad, San Diego, CA, USA). Kaplan−Meier plots were created by using GraphPad Prism software (GraphPad). The statistical significance was analyzed by the log-rank (Mantel−Cox) test. A p value of <0.05 was considered statistically significant.

■ ASSOCIATED CONTENT

Supporting Information

The Supporting Information is available free of charge on the ACS Publications website at DOI: 10.1021/acsami.5b04905.

Methods and supplementary figures S1−S14 (PDF)

■ AUTHOR INFORMATION

Corresponding Authors

*(P.P.M.) E-mail: pp_manna@yahoo.com.

*(B.R.) E-mail: biswajitray2003@yahoo.co.in.

Author Contributions

‖S.K.H. and K.R. contributed equally.

Notes

The authors declare no competing financial interest.

■ ACKNOWLEDGMENTS

The present work was supported by grants from the Department of Biotechnology (DBT), New Delhi, India, No. BT/PR11490/BRB/10/675/2008 (PPM) and BT/PR889/NNT/28/570/2011 (B.R. and P.P.M.). K.R. gratefully acknowledges IIT (BHU), Varanasi, India, for a teaching assistantship. We thank Dr. M. Yashpal, IMS, BHU, for providing the TEM facilities. We thank Prof. Sanjay Singh, Department of Pharmaceutics, IIT (BHU), for providing the methotrexate drug.

■ REFERENCES

(1) Gaucher, G.; Dufresne, M.-H.; Sant, V. P.; Kang, N.; Maysinger, D.; Leroux, J.-C. Block Copolymer Micelles: Preparation, Characterization and Application in Drug Delivery. *J. Controlled Release* **2005**, *109*, 169−188.

DOI: 10.1021/acsami.5b04905
ACS Appl. Mater. Interfaces 2015, 7, 20021−20033

(2) Lavasanifar, A.; Samuel, J.; Kwon, G. S. Poly(Ethylene Oxide)-Block-Poly(L-Amino Acid) Micelles for Drug Delivery. *Adv. Drug Delivery Rev.* **2002**, *54*, 169−190.
(3) Oh, J. K. Polylactide (Pla)-Based Amphiphilic Block Copolymers: Synthesis, Self-Assembly, and Biomedical Applications. *Soft Matter* **2011**, *7*, 5096−5108.
(4) Stenzel-Rosenbaum, M. H.; Davis, T. P.; Fane, A. G.; Chen, V. Porous Polymer Films and Honeycomb Structures Made by the Self-Organization of Well-Defined Macromolecular Structures Created by Living Radical Polymerization Techniques. *Angew. Chem., Int. Ed.* **2001**, *40*, 3428−3432.
(5) Huh, J.; Kim, K. H.; Ahn, C.-H.; Jo, W. H. Micellization Behavior of Star-Block Copolymers in a Selective Solvent: A Brownian Dynamics Simulation Approach. *J. Chem. Phys.* **2004**, *121*, 4998−5004.
(6) Bilalis, P.; Pitsikalis, M.; Hadjichristidis, N. Controlled Nitroxide-Mediated and Reversible Addition−Fragmentation Chain Transfer Polymerization of N-Vinylpyrrolidone: Synthesis of Block Copolymers with Styrene and 2-Vinylpyridine. *J. Polym. Sci., Part A: Polym. Chem.* **2006**, *44*, 659−665.
(7) Heise, A.; Hedrick, J. L.; Frank, C. W.; Miller, R. D. Starlike Block Copolymers with Amphiphilic Arms as Models for Unimolecular Micelles. *J. Am. Chem. Soc.* **1999**, *121*, 8647−8648.
(8) Mishra, A. K.; Patel, V. K.; Vishwakarma, N. K.; Biswas, C. S.; Raula, M.; Misra, A.; Mandal, T. K.; Ray, B. Synthesis of Well-Defined Amphiphilic Poly(E-Caprolactone)-B-Poly(N-Vinylpyrrolidone) Block Copolymers Via the Combination of Rop and Xanthate-Mediated Raft Polymerization. *Macromolecules* **2011**, *44*, 2465−2473.
(9) Mishra, A.; Ramesh, K.; Paira, T.; Srivastava, D.; Mandal, T.; Misra, N.; Ray, B. Synthesis and Self-Assembly Properties of Well-Defined Four-Arm Star Poly(E-Caprolactone)-B-Poly(N-Vinylpyrrolidone) Amphiphilic Block Copolymers. *Polym. Bull.* **2013**, *70*, 3201−3220.
(10) Wan, D.; Satoh, K.; Kamigaito, M.; Okamoto, Y. Xanthate-Mediated Radical Polymerization of N-Vinylpyrrolidone in Fluoroalcohols for Simultaneous Control of Molecular Weight and Tacticity. *Macromolecules* **2005**, *38*, 10397−10405.
(11) Ray, B.; Kotani, M.; Yamago, S. Highly Controlled Synthesis of Poly(N-Vinylpyrrolidone) and Its Block Copolymers by Organostibine-Mediated Living Radical Polymerization. *Macromolecules* **2006**, *39*, 5259−5265.
(12) Yamago, S.; Kayahara, E.; Kotani, M.; Ray, B.; Kwak, Y.; Goto, A.; Fukuda, T. Highly Controlled Living Radical Polymerization through Dual Activation of Organobismuthines. *Angew. Chem., Int. Ed.* **2007**, *46*, 1304−1306.
(13) Lu, X.; Gong, S.; Meng, L.; Li, C.; Yang, S.; Zhang, L. Controllable Synthesis of Poly(N-Vinylpyrrolidone) and Its Block Copolymers by Atom Transfer Radical Polymerization. *Polymer* **2007**, *48*, 2835−2842.
(14) Patel, V.; Mishra, A.; Vishwakarma, N.; Biswas, C.; Ray, B. (S)-2-(Ethyl Propionate)-(O-Ethyl Xanthate) and (S)-2-(Ethyl Isobutyrate)-(O-Ethyl Xanthate)-Mediated Raft Polymerization of N-Vinylpyrrolidone. *Polym. Bull.* **2010**, *65*, 97−110.
(15) Le Garrec, D.; Gori, S.; Luo, L.; Lessard, D.; Smith, D. C.; Yessine, M. A.; Ranger, M.; Leroux, J. C. Poly(N-Vinylpyrrolidone)-Block-Poly(D,L-Lactide) as a New Polymeric Solubilizer for Hydrophobic Anticancer Drugs: In Vitro and in Vivo Evaluation. *J. Controlled Release* **2004**, *99*, 83−101.
(16) Gaucher, G.; Asahina, K.; Wang, J.; Leroux, J.-C. Effect of Poly(N-Vinyl-Pyrrolidone)-Block-Poly(D,L-Lactide) as Coating Agent on the Opsonization, Phagocytosis, and Pharmacokinetics of Biodegradable Nanoparticles. *Biomacromolecules* **2009**, *10*, 408−416.
(17) Luo, L.; Ranger, M.; Lessard, D. G.; Le Garrec, D.; Gori, S.; Leroux, J.-C.; Rimmer, S.; Smith, D. Novel Amphiphilic Diblock Copolymer of Low Molecular Weight Poly(N-Vinylpyrrolidone)-Block-Poly(D,L-Lactide): Synthesis, Characterization, and Micellization. *Macromolecules* **2004**, *37*, 4008−4013.
(18) Ramesh, K.; Mishra, A. K.; Patel, V. K.; Vishwakarma, N. K.; Biswas, C. S.; Paira, T. K.; Mandal, T. K.; Maiti, P.; Misra, N.; Ray, B. Synthesis of Well-Defined Amphiphilic Poly(D,L-Lactide)-B-Poly(N-Vinylpyrrolidone) Block Copolymers Using Rop and Xanthate-Mediated Raft Polymerization. *Polymer* **2012**, *53*, 5743−5753.
(19) Lin, Y.; Zhang, A. Synthesis and Characterization of Star-Shaped Poly(D,L-Lactide)-Block-Poly(Ethylene Glycol) Copolymers. *Polym. Bull.* **2010**, *65*, 883−892.
(20) Wei, H.; Chen, W.-Q.; Chang, C.; ChengCheng; Cheng, S.-X.; Zhang, X.-Z.; Zhuo, R.-X. Synthesis of Star Block, Thermosensitive Poly(L-Lactide)-Star Block-Poly(N-Isopropylacrylamide-Co-N-Hydroxymethylacrylamide) Copolymers and Their Self-Assembled Micelles for Controlled Release. *J. Phys. Chem. C* **2008**, *112*, 2888−2894.
(21) Li, J.; Ren, J.; Cao, Y.; Yuan, W. Synthesis of Biodegradable Pentaarmed Star-Block Copolymers Via an Asymmetric Bis-Tris Core by Combination of Rop and Raft: From Star Architectures to Double Responsive Micelles. *Polymer* **2010**, *51*, 1301−1310.
(22) Fischer, A. M.; Thiermann, R.; Maskos, M.; Frey, H. One-Pot Synthesis of Poly(L-Lactide) Multi-Arm Star Copolymers Based on a Polyester Polyol Macroinitiator. *Polymer* **2013**, *54*, 1993−2000.
(23) Kang, N.; Leroux, J.-C. Triblock and Star-Block Copolymers of N-(2-Hydroxypropyl)Methacrylamide or N-Vinyl-2-Pyrrolidone and D,L-Lactide: Synthesis and Self-Assembling Properties in Water. *Polymer* **2004**, *45*, 8967−8980.
(24) Kukowska-Latallo, J. F.; Candido, K. A.; Cao, Z.; Nigavekar, S. S.; Majoros, I. J.; Thomas, T. P.; Balogh, L. P.; Khan, M. K.; Baker, J. R. Nanoparticle Targeting of Anticancer Drug Improves Therapeutic Response in Animal Model of Human Epithelial Cancer. *Cancer Res.* **2005**, *65*, 5317−5324.
(25) Mauldin, R. V.; Carroll, M. J.; Lee, A. L. Dynamic Dysfunction in Dihydrofolate Reductase Results from Antifolate Drug Binding: Modulation of Dynamics within a Structural State. *Structure* **2009**, *17*, 386−394.
(26) Dendooven, A.; De Rycke, L.; Verhelst, X.; Mielants, H.; Veys, E. M.; De Keyser, F. Leflunomide and Methotrexate Combination Therapy in Daily Clinical Practice. *Ann. Rheum. Dis.* **2006**, *65*, 833−834.
(27) Feazell, R. P.; Nakayama-Ratchford, N.; Dai, H.; Lippard, S. J. Soluble Single-Walled Carbon Nanotubes as Longboat Delivery Systems for Platinum(Iv) Anticancer Drug Design. *J. Am. Chem. Soc.* **2007**, *129*, 8438−8439.
(28) Tassa, C.; Duffner, J. L.; Lewis, T. A.; Weissleder, R.; Schreiber, S. L.; Koehler, A. N.; Shaw, S. Y. Binding Affinity and Kinetic Analysis of Targeted Small Molecule-Modified Nanoparticles. *Bioconjugate Chem.* **2010**, *21*, 14−19.
(29) Klein, E.; Klein, G. Differential Survival of Solid Tumor Cells after Inoculation into Established Ascites Tumors. *Cancer Res.* **1954**, *14*, 139−144.
(30) Hussain, H.; Tan, B. H.; Gudipati, C. S.; Liu, Y.; He, C. B.; Davis, T. P. Synthesis and Self-Assembly of Poly(Styrene)-B-Poly(N-Vinylpyrrolidone) Amphiphilic Diblock Copolymers Made Via a Combined Atrp and Madix Approach. *J. Polym. Sci., Part A: Polym. Chem.* **2008**, *46*, 5604−5615.
(31) Zhang, Y.; Jin, T.; Zhuo, R.-X. Methotrexate-Loaded Biodegradable Polymeric Micelles: Preparation, Physicochemical Properties and in Vitro Drug Release. *Colloids Surf., B* **2005**, *44*, 104−109.
(32) Sun, H.; Guo, B.; Li, X.; Cheng, R.; Meng, F.; Liu, H.; Zhong, Z. Shell-Sheddable Micelles Based on Dextran-Ss-Poly(E-Caprolactone) Diblock Copolymer for Efficient Intracellular Release of Doxorubicin. *Biomacromolecules* **2010**, *11*, 848−854.
(33) Torchilin, V. Tumor Delivery of Macromolecular Drugs Based on the Epr Effect. *Adv. Drug Delivery Rev.* **2011**, *63*, 131−135.
(34) Hira, S. K.; Mondal, I.; Bhattacharya, D.; Manna, P. P. Downregulation of Endogenous Stat3 Augments Tumoricidal Activity of Interleukin 15 Activated Dendritic Cell against Lymphoma and Leukemia Via Trail. *Exp. Cell Res.* **2014**, *327*, 192−208.
(35) Ohnoshi, T.; Ohnuma, T.; Takahashi, I.; Scanlon, K.; Kamen, B. A.; Holland, J. F. Establishment of Methotrexate-Resistant Human Acute Lymphoblastic Leukemia Cells in Culture and Effects of Folate Antagonists. *Cancer Res.* **1982**, *42*, 1655−1660.

DOI: 10.1021/acsami.5b04905
ACS Appl. Mater. Interfaces 2015, 7, 20021−20033

(36) Hira, S. K.; Mishra, A. K.; Ray, B.; Manna, P. P. Targeted Delivery of Doxorubicin-Loaded Poly (Epsilon-Caprolactone)-B-Poly(N-Vinylpyrrolidone) Micelles Enhances Antitumor Effect in Lymphoma. *PLoS One* **2014**, *9*, e94309.
(37) Kuznetsova, N. R.; Sevrin, C.; Lespineux, D.; Bovin, N. V.; Vodovozova, E. L.; Mészáros, T.; Szebeni, J.; Grandfils, C. Hemocompatibility of Liposomes Loaded with Lipophilic Prodrugs of Methotrexate and Melphalan in the Lipid Bilayer. *J. Controlled Release* **2012**, *160*, 394−400.
(38) Manna, P. P.; Hira, S. K.; Das, A. A.; Bandyopadhyay, S.; Gupta, K. K. Il-15 Activated Human Peripheral Blood Dendritic Cell Kill Allogeneic and Xenogeneic Endothelial Cells Via Apoptosis. *Cytokine+* **2013**, *61*, 118−126.

DOI: 10.1021/acsami.5b04905
ACS Appl. Mater. Interfaces 2015, 7, 20021−20033